Ke Ai
ADVANCING RESEARCH
EVOLVING SCIENCE

CrossMark

Available online at www.sciencedirect.com

ScienceDirect

Journal of Natural Gas Geoscience 1 (2016) 397–406

http://www.keaipublishing.com/jnggs

Original research paper

A new method in predicting productivity of multi-stage fractured horizontal well in tight gas reservoirs☆

Yunsheng Wei*, Ailin Jia, Dongbo He, Junlei Wang

Research Institute of Petroleum Exploration & Development, PetroChina, Beijing 100083, China

Received 3 August 2016; revised 28 September 2016
Available online 27 October 2016

Abstract

The generally accomplished technique for horizontal wells in tight gas reservoirs is by multi-stage hydraulic fracturing, not to mention, the flow characteristics of a horizontal well with multiple transverse fractures are very intricate. Conventional methods, well as an evaluation unit, are difficult to accurately predict production capacity of each fracture and productivity differences between wells with a different number of fractures. Thus, a single fracture sets the minimum evaluation unit, matrix, fractures, and lateral wellbore model that are then combined integrally to approximate horizontal well with multiple transverse hydraulic fractures in tight gas reservoirs. This paper presents a new semi-analytical methodology for predicting the production capacity of a horizontal well with multiple transverse hydraulic fractures in tight gas reservoirs. Firstly, a mathematical flow model used as a medium, which is disturbed by finite conductivity vertical fractures and rectangular shaped boundaries, is established and explained by the Fourier integral transform. Then the idea of a single stage fracture analysis is incorporated to establish linear flow model within a single fracture with a variable rate. The Fredholm integral numerical solution is applicable for the fracture conductivity function. Finally, the pipe flow model along the lateral wellbore is adapted to couple multi-stages fracture mathematical models, and the equation group of predicting productivity of a multi-stage fractured horizontal well. The whole flow process from the matrix to bottom-hole and production interference between adjacent fractures is also established. Meanwhile, the corresponding iterative algorithm of the equations is given. In this case analysis, the productions of each well and fracture are calculated under the different bottom-hole flowing pressure, and this method also contributes to obtaining the distribution of pressure drop and production for every horizontal segment and its changes with effective fracture half-length and conductivity. Application of this technology will provide gas reservoir engineers a better tool to predict well and fracture productivity, besides optimizing transverse hydraulic fractures configuration and conductivity along the lateral wellbore.

Keywords: Tight gas; Multi-stage hydraulically fractured horizontal well; Single fracture; Production interference between adjacent fractures; Productivity prediction

1. Introduction

There are many transverse fractures with different forms around a horizontal well after being fractured multi-stage in tight gas reservoirs, this greatly increases the contact area a between gas well and the formation. Simultaneously, the flow conditions around the bottom-hole are improved. The states of gas flow include Darcy flow in the formation pores, variable Darcy flow in the hydraulic fractures, and variable pipe flow in

☆ This is English translational work of an article originally published in *Natural Gas Geoscience* (in Chinese).The original article can be found at: 10.11764/j.issn.1672-1926.2016.06.1101.

* Corresponding author.
E-mail address: weiys@petrochina.com.cn (Y. Wei).

Peer review under responsibility of Editorial office of *Journal of Natural Gas Geoscience*.

http://dx.doi.org/10.1016/j.jnggs.2016.10.004

the horizontal wellbore. The interferences and the coupling happen between the three flow patterns by means of the boundary conditions.

In terms of research on finite conductivity fractures, parts [1] unraveled the flow relationship between the elliptic fractures and matrix by conformal transformation; this presented the function relationship between finite conductivity and effective wellbore diameter. Cinco-Ley [2] evaluated the flow capacity of fractures with finite conductivity by the numerical discrete method. Liao [3] researched variable flow within fractures through transforming elliptic coordinate. On these bases, the analysis on unstable flow of fractured horizontal well within closed formation, Zerzar [4] obtained the characteristics of a linear (double) flow in the early stages, and a quasi-steady flow in the late stages done by the gradual approximation method; the parameters of the fractured horizontal well were then analyzed. Brown [5] used three linear flow models to reflect the flow law within the hydraulic fracture, the inner reservoir between hydraulic fractures, and the outer reservoir away from the tips of the fracture system. Regarding the productivity evaluation of fractured horizontal wells, based on the Joshi [6,7] productivity formula, Raghavan [8] introduced a method of predicting productivity of a multi-stage fractured horizontal well, which substitutes the equivalent wellbore radius (radial flow) for hydraulic fractures to simulate fluid flow. Wang [9] corrected the equivalent wellbore diameter of the horizontal wells with vertical rectangular fractures through introducing the influence function of finite conductivity fractures. Meanwhile, in combination with pressure superposition principle, the influence factors of fractured horizontal well productivity were evaluated. Wang [10] established the mathematical model flow of a multi-stage fractured horizontal well; the characteristics include the rectangular closed boundary by means of the two variables considering gas slippage, the pseudo-pressure, and the pseudo-time. Based on the wellbore with infinite conductivity, the change on horizontal well productivity is analyzed with the various fracture length, fracture conductivity, the number of fractures, fractured horizontal well length, and so on. Li [11] established the empirical plate to evaluate the open flow rate and cumulative production based on demonstrating the scale of the effective sand. Li [12] quickly evaluated the horizontal well productivity in low-permeability and tight gas reservoirs through combining ideal model with numerical simulation. In this paper, with the aid of previous research study results, the idea [13] of a single fracture is introduced to accurately evaluate the productivity of fractured horizontal wells in tight gas reservoirs. By a single fracture serving as a unit, the principle of mass conservation is applied to couple the elliptic flow in a typical reservoir, as well as variable flow within fractures and variable pipe flow in the horizontal wellbore. Meanwhile, considering the interference between the adjacent fractures, the theoretical formula, and the corresponding algorithm are established for predicting productivity of fractured horizontal wells; the practical examples are analyzed for model verification. Thus, a new method for predicting productivity of multi-stage fractured horizontal wells in a tight gas reservoir is formed.

2. Mathematical model

2.1. Flow model in formation with finite conductivity fracture

There are complex flow types in the reservoir with fractures. The gas in pores flow linearly into fractures across the surface, the streamline form within limit scope around fractures and is similar to an elliptic flow, and pseudo-radial flow is usually expressed out of the elliptic flow (Fig. 1).

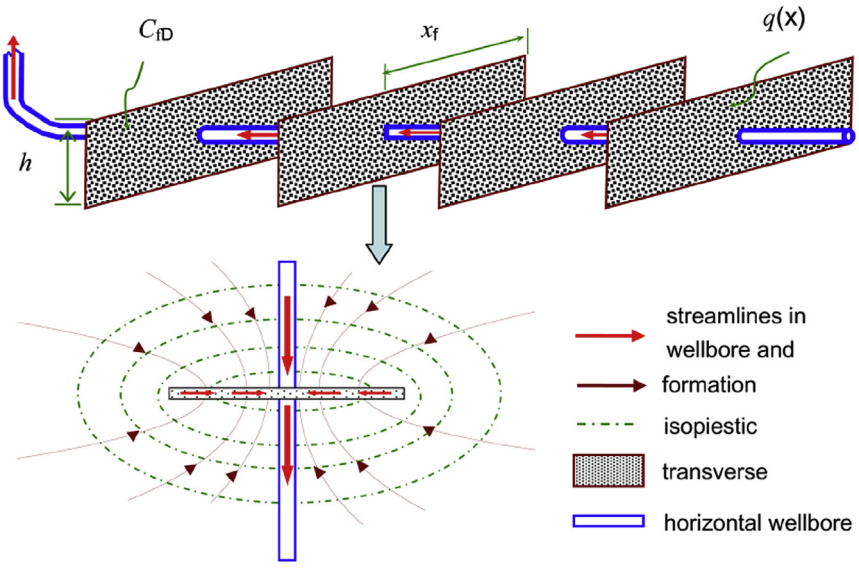

Fig. 1. Multi-stage fractured horizontal well and single fracture flow.

Fracture conductivity has a great impact on gas well productivity in tight gas reservoirs. For that reason, the flow in the fracture is not negligible. In order to quantitatively describe the flow characteristics of fractures, some idealizations and simplifying were made assuming the following:

(1) The formation is homogeneous, and there's uniform thickness at the top and bottom.
(2) The fractures do not drain beyond the boundaries of this rectangular geometry ($x_e \times y_e$) with constant pressure.
(3) The perforated thickness of the fractures, h, is the same as the thickness of the reservoir. Furthermore, $q(x)$ is the variable for the length of the fracture.

Definitions of the dimensionless variables are as follows:

$$P_D = \frac{0.0786kh\left(P_i^2 - P^2\right)}{\mu ZTQ_{sc}},\ q_D = \frac{2x_f q(x)}{Q_{sc}},\ j_D = \frac{j}{x_f}(j = x, y),\ C_{fD} = \frac{k_f w_f}{kx_f}$$

The dimensionless control equation and the associated boundary conditions for the formation around fractures are given:

$$\frac{\partial^2 P_D}{\partial x_D^2} + \frac{\partial^2 P_D}{\partial y_D^2} + q_D(x_D)\delta(y_D - y_{wD}) = 0 \tag{1}$$

$$P_D(x_D, 0) = P_D(x_D, x_{eD}) \tag{2}$$

and

$$P_D(0, y_D) = P_D(y_{eD}, y_D) \tag{3}$$

wherein x_w, y_w are the coordinates of the fracture center, $\boldsymbol{\delta}$ is the Dirac function.

In Eq. (1), Fourier finite sine integral of P_D and q_D along the direction of x_D and y_D are given, respectively, by

$$\widehat{P}_D = \int_0^{x_{eD}} P_D \sin(\beta_m x_D) dx_D \tag{4}$$

$$\overline{P}_D = \int_0^{y_{eD}} P_D \sin(\gamma_n y_D) dy_D \tag{5}$$

and

$$\tilde{q}_D = \int_0^{x_{eD}} q_D(x_D)\sin(\gamma_n x_D) dx_D \tag{6}$$

where the over-bar symbol indicates various integral transform direction.

The relationship between the dimensionless pressure through the double Fourier integral transform and dimensionless fracture production is given, depending on the boundary conditions Eqs. (2) and (3), by means of

$$-\pi^2\left(\frac{m^2}{x_{eD}^2} + \frac{n^2}{y_{eD}^2}\right)\widehat{\overline{P}}_D + \tilde{q}_D \sin\gamma_n y_{wD} = 0 \tag{7}$$

The dimensionless pressure is obtained from Eq. (7) by two inverse transformations as follows:

$$P_D = \sum_{n=1}^{\infty} \frac{\sin(\gamma_n y_D)}{N(\beta_n)} \left(\sum_{m=1}^{\infty} \frac{\sin(\beta_m x_D)}{N(\beta_m)} \widehat{\overline{P}}_D \right) \tag{8}$$

where the eigenvalues are given by

$$\beta_m = m\pi/x_{eD};\ \gamma_n = n\pi/y_{eD} \tag{9}$$

and the bottom of the norms is given by

$$N(\beta_m) = \int_0^{x_{eD}} \sin^2(\beta_m x_D) dx_D = \frac{x_{eD}}{2};$$
$$N(\gamma_n) = \int_0^{y_{eD}} \sin^2(\gamma_n y_D) dy_D = \frac{y_{eD}}{2} \tag{10}$$

To substitute Eqs. (7), (9) and (10) into Eq. (8), the formula for pressure is obtained as follows:

$$P_D = \sum_{m=1}^{\infty} \frac{2\tilde{q}_D}{x_{eD} y_{eD}} \sin\frac{m\pi x_D}{x_{eD}} \left[\sum_{n=1}^{\infty} \frac{\cos n\pi(y_D - y_{wD})/y_{eD} - \cos n\pi(y_D + y_{wD})/y_{eD}}{\pi^2(m^2/x_{eD}^2 + n^2/y_{eD}^2)} \right] \tag{11}$$

Assuming that there's only flux distribution along the fractures, Eq. (6) becomes

$$\tilde{q}_D = \int_{x_{wD}-1}^{x_{wD}+1} q_D(\alpha)\sin\left(\frac{m\pi\alpha}{x_{eD}}\right) d\alpha \tag{12}$$

and the transformation is as follows:

$$\sum_{k=1}^{\infty} \frac{\cos k\pi x}{k^2 + a^2} = \frac{\pi}{2a} \frac{\cosh[a\pi(1-x)]}{\sinh(a\pi)} - \frac{1}{2a^2};\ [0 \le x \le 2\pi] \tag{13}$$

The solution of the pressure at the intersection point (x_{wD},y_{wD}) of the horizontal wellbore and finite conductivity

fractures can be obtained after commencing Eq. (11)–(13) as follows:

$$P_D(x_D,y_D;x_{wD},y_{wD})=2\int_{x_{wD}-1}^{x_{wD}+1}\left\{\sum_{m=1}^{\infty}\frac{q_D(\alpha)}{m\pi}\sin\frac{m\pi x_D}{x_{eD}}\sin\frac{m\pi\alpha}{x_{eD}}\frac{\cosh\frac{m\pi(y_{eD}-|y_D-y_{wD}|)}{x_{eD}}-\cosh\frac{m\pi(y_{eD}-|y_D+y_{wD}|)}{x_{eD}}}{\sinh\frac{m\pi y_{eD}}{x_{eD}}}\right\}d\alpha \tag{14}$$

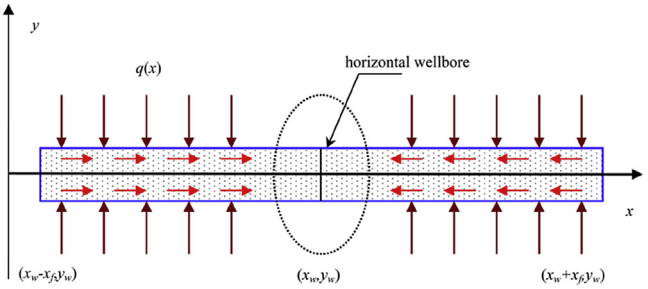

Fig. 2. Variable rate of linear flow in fractures.

The coupling conditions between the fracture and the formation are given by

$$P_{fD}(x_D)=P_D(x_D,y_{wD};x_{wD},y_{wD}),\ [-1\le x_D\le 1] \tag{18}$$

The Fredholm integral equation is obtained by substituting Eq. (14) with Eq. (18). Then again this equation can't be solved by means of an analytical method. The numerical method is given as follows: the fracture is divided evenly into n sections and the flux and pressure of each section are uniform. Thus, we can obtain n + 1 order equations (Eq. (19)) about the flux at each section, q_{Dj} (j = 1,2,3 …. ,n), and the bottom-hole pressure, P_{wD}.

where the flux constraint equation is given as follows:

$$\begin{aligned}&P_{wD}+2\sum_{i=1}^{n}q_{Di}\sum_{m=1}^{\infty}\left\{\begin{array}{l}\frac{x_{eD}}{m^2\pi^2}\sin m\pi\frac{x_{wD}+(j-0.5)\Delta x}{x_{eD}}\left[\cos m\pi\frac{x_{wD}+i\Delta x_D}{x_{eD}}-\cos m\pi\frac{x_{wD}+(i-1)\Delta x_D}{x_{eD}}\right]\\ \times\frac{\cosh[m\pi y_{eD}/x_{eD}]-\cosh[m\pi(y_{eD}-|2y_{wD}|)/x_{eD}]}{\sinh(m\pi y_{eD}/x_{eD})}\end{array}\right\}\\&=\frac{\pi}{C_{fD}}\left\{(x_{wD}+(j-0.5)\Delta x)\left(1-\sum_{i=1}^{j-1}q_{Di}\Delta x_D-\frac{\Delta x_D}{2}q_{Dj}\right)+\sum_{i=1}^{j-1}q_{Di}\Delta x_D[x_{wD}+(i-0.5)\Delta x_D]+q_{Dj}\Delta x_D\frac{x_{wD}+(j-0.75)\Delta x_D}{2}\right\}\end{aligned} \tag{19}$$

2.2. Flow model in finite conductivity fracture

Flow within fracture is assumed to be one-dimensional linear flow with a variable rate in the x direction (Fig. 2).

The elastic energy in the fracture is ignored because the volume of the fracture is minute. The dimensionless flow equation within the hydraulic fracture can be simplified to stabilize the state equation as follows:

$$\frac{d^2P_{fD}}{dx_D^2}+\frac{2}{C_{fD}}q_D(x_D)=0,\ [-1\le x_D\le 1] \tag{15}$$

The inner boundary condition is given by

$$\frac{dP_{fD}(x_{wD})}{dx_D}=-\frac{\pi}{C_{fD}} \tag{16}$$

After the second integral to x_D, Eq. (15) becomes

$$P_{wD}-P_{fD}(x_D)=\frac{\pi}{C_{fD}}\left[|x_D-x_{wD}|-\int_{x_{wD}}^{x_D}dv\int_{x_{wD}}^{v}q_D(u)du\right] \tag{17}$$

$$\sum_{i=1}^{n}q_{Di}=1 \tag{20}$$

The Newton iteration is used to solve Eq. (19). Meanwhile, the relationship between the dimensionless conductivity C_{fD} and the dimensionless bottom-hole pressure P_{wD} are analyzed

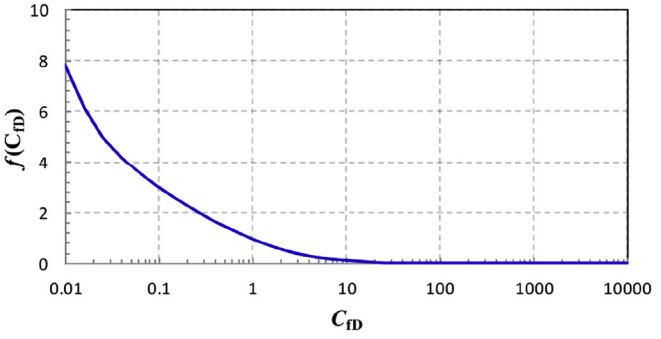

Fig. 3. Relationships between finite conductivity fracture influence function and dimensionless conductivity.

under diverse outer boundary conditions. The results indicate that the dimensionless bottom-hole pressure P_{wD} decreases with the increase of the C_{fD} in the finite conductivity fracture. Whenever $C_{fD} > 1000$, P_{wD} tends to be constant, hence, P_{infwD}, which is the dimensionless bottom-hole pressure in the infinite conductivity fracture; this trend is only related to C_{fD}. Through data regression, the differential function, $f(C_{fD})$, that is, the influence function of fracture conductivity is obtained through Eq. (21). Kindly refer to Fig. 3.

$$f(C_{fD}) = \frac{0.95 - 0.56u + 0.16u^2 - 0.028u^3 + 0.0028u^4 - 0.00011u^5}{1.0 + 0.094u + 0.093u^2 + 0.0084u^3 + 0.001u^4 + 0.00036u^5},\ u = \ln C_{fD} \tag{21}$$

where the dimensionless bottom-hole pressure in the infinite conductivity fracture is given by

$$P_{\mathrm{inf}wD} = 2\left\{ \sum_{n=1}^{\infty} \frac{x_{eD}}{n^2\pi} \sin n\pi \frac{x_D}{x_{eD}} \sin n\pi \frac{1}{x_{eD}} \sin n\pi \frac{x_{wD}}{x_{eD}} \frac{\cosh \frac{n\pi y_{eD}}{x_{eD}} - \cosh \frac{n\pi (y_{eD} - 2y_{wD})}{x_{eD}}}{\sinh \frac{n\pi y_{eD}}{x_{eD}}} \right\} \tag{22}$$

In the subsequent derivations, the one-dimensional (linear) flow has been assumed within the hydraulic fracture; that is, the radial convergence of flow towards the wellbore has been ignored within the hydraulic fracture. Nonetheless, the radial flow near the horizontal wellbore exists objectively. Therefore, the skin factor is introduced to calculate the flow resistance. The formula Ref. [9] is given:

$$skin = \frac{kh}{k_f w_f} \left[\ln \frac{h}{2r_w} - \frac{\pi}{2} \right] \tag{23}$$

Adding the choking skin to Eq. (22), we obtain the following solution. This is a good approximation for dimensionless wellbore pressure after the end of radial flow in the finite conductivity fracture:

$$P_{finwD} = P_{\mathrm{inf}wD} + f(C_{fD}) + skin \tag{24}$$

That is:

$$\frac{P_i^2 - P_{wf}^2}{Q_{sc}} = \frac{\mu ZT}{0.0786kh} \left\{ \begin{array}{l} \frac{1}{C_{fD}} \frac{h}{x_f} \left[\ln \frac{h}{2r_w} - \frac{\pi}{2} \right] + f(C_{fD}) \\ +2 \sum_{m=1}^{\infty} \left[\frac{x_e}{m^2 \pi x_f} \sin \frac{m\pi x_f}{x_e} \sin^2 \frac{m\pi x_w}{x_e} \frac{\cosh \frac{m\pi y_e}{x_e} - \cosh \frac{m\pi (y_e - 2y_w)}{x_e}}{\sinh \frac{m\pi y_e}{x_e}} \right] \end{array} \right\} \tag{25}$$

Using Eq. (25), the productivity of a single transverse fracture with finite conductivity can be quickly calculated. The calculation is the basis for predicting productivity of a multi-stage fractured horizontal well.

2.3. Horizontal wellbore model

Multiple transverse hydraulic fractures are coupled with each other through the pipe flow in the horizontal wellbore.

The single-phase pipe flow is considered because the diameter of horizontal wellbore is far greater than the size of the flow channel in the formation and fracture. Flow rate in the horizontal wellbore is changing, hence, the flow pressure is calculated piecewise. The pressure gradient [14] is given by

$$\frac{dP}{dy} = f \frac{\rho v^2}{2r_w} \tag{26}$$

where the pressure drop of the kinetic energy is caused by the increase in velocity is ignored.

Through separating variables and definite integral based on Eq. (26), the relationship between the gas flow rate and pressure square difference is derived as follows:

$$P_{wfi}^2 - P_{wfi-1}^2 = 9 \times 10^{-12} \frac{ZT\gamma_g}{r_w^5} f_i d_i \left(\sum_{j=i}^{n} Q_{scj} \right)^2 \quad (i = 1, 2, \cdots, n; P_{wf0} = P_{wf}) \tag{27}$$

where f is calculated by Eq. (28), in which the Reynolds number considering the turbulent condition is calculated by means of Eq. (29).

$$f_i = \left[1.14 - 2\lg\left(\frac{e}{1000D} + \frac{21.25}{R_{ei}^{0.9}}\right)\right]^{-2} \tag{28}$$

and

$$R_{ei} = \frac{177.1\gamma_g \sum_{j=i}^{n} Q_{scj}}{2\mu r_w} \tag{29}$$

2.4. Productivity model with the interference between adjacent fractures

The interference [15,16] between adjacent fractures happens very often when the steady state flow or pseudo-steady state flow appears. For the quantitative evaluation to be easy, the interference degree, the outer flow boundary for every fracture is described as an elliptic boundary.

The flow resistance from outer boundary to horizontal wellbore is given by:

$$R = \frac{\mu ZT}{0.0786kh} \ln\frac{\sqrt{ab}}{r_{we}} \tag{30}$$

where a, b is the semi-major axis and semi-minor axis of outer boundary elliptic, respectively, m; r_{we} is equivalent radius, m, and the formula Ref. [17]–[19] is given by:

$$r_{we} = 2x_f \exp\left\{-\left[\frac{3}{2} + f(C_{fD}) + skin\right]\right\} \tag{31}$$

In combining Eq. (25) with Eqs. (30) and (32) is obtained by:

$$\ln\frac{\sqrt{ab}}{r_{we}} = \frac{1}{C_{fD}}\frac{h}{x_f}\left[\ln\frac{h}{2r_w} - \frac{\pi}{2}\right] + f(C_{fD}) + 2\sum_{m=1}^{\infty}\left[\frac{x_e}{m^2\pi x_f}\sin\frac{m\pi x_f}{x_e}\sin^2\frac{m\pi x_w}{x_e}\frac{\cosh\frac{m\pi y_e}{x_e} - \cosh\frac{m\pi(y_e-2y_w)}{x_e}}{\sinh\frac{m\pi y_e}{x_e}}\right] \tag{32}$$

where

$$a^2 - b^2 = x_f^2. \tag{33}$$

The elliptic boundary size and shape of every fracture can be calculated by means of Eq. (32) and Eq. (33) where every fracture spatial location is combined. The interference of every fracture outer flow boundary is then determined (Fig. 4).

Assuming the flow area of every fracture is respectively A_1, A_2, …… A_n, the intersecting area of adjacent elliptic boundary is respectively B_{12}, B_{21}, B_{23}, B_{32}, ……$B_{(n-1)n}$, $B_{n\,(n-1)}$, and the production rate of every fracture is Q_{sc1}, Q_{sc1}, ……Q_{scn} when the interference between the adjacent fracture is not considered. According to the principle of flow area [20,21], every fractures' contribution to the horizontal well production

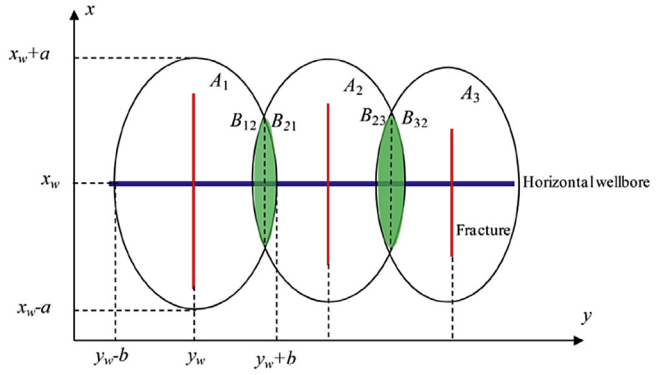

Fig. 4. Scheme with interference between fractures in fractured horizontal well.

is proportional to its area of flow boundary; then the actual production rate of every fracture is acquired:

$$Q_{scr1} = \frac{A_1 - B_{21}}{A_1} Q_{sc1}$$

$$Q_{scri} = \frac{A_i - B_{(i-1)i} - B_{(i+1)i}}{A_i} Q_{sci} \quad (1 < i < n) \tag{34}$$

$$Q_{scrn} = \frac{A_n - B_{(n-1)n}}{A_n} Q_{scn}$$

then the production rate of the fractured horizontal well is given by:

$$Q_{scrt} = \sum_{i=1}^{n} Q_{scri} \tag{35}$$

By means of Eq. (25) and Eq. (34), the bottom-hole pressure of every fracture and the distribution of pressure in a horizontal wellbore are obtained.

3. Model solution

Assuming the number of hydraulic fractures, n, Eq. (27) is a nonlinear equation which can be used to quickly and accurately solve the numerical iteration. The steps are as follows:

Step 1: The flow rates of the nth fracture, Q_{scnmax} and Q_{scnmin}, are assumed, therefore, Q_{scnmid}=(Q_{scnmax} + Q_{scnmin})/2.

Prior Step 2 and 3, the pressure points of the nth fracture across the horizontal wellbore, $P_{wfnmax(0)}$, $P_{wfnmin(0)}$, $P_{wfnmid(0)}$, are calculated.

Step 2: The flow rate of the (n−1)th fracture, Q_{scn-1} is calculated on the basis of Eqs. (25) and (27).
Step 3: According to Step 2, the flow rates of the i_{th} fracture are calculated in turn. When that of the first fracture is calculated, the pressure values of the first fracture across the horizontal wellbore, $P_{wf1max(0)}$, $P_{wf1min(0)}$, $P_{wf1mid(0)}$, can be calculated directly.
Step 4: If $(P_{wf1max(0)}\text{-}P_{wf}) \times (P_{wf1mid(0)}\text{-}P_{wf})<0$, then $Q_{scnmin} = Q_{scnmid}$, or $Q_{scnmax} = Q_{scnmid}$.
Step 5: Step 2 to Step 4 are not looped until the precision of $P_{wfmid(j)}$ is fulfilled.

Through the preceding steps and the corresponding computer program, the flow rate of every fracture not considering the interference between adjacent fractures is obtained.

Step 6: Combining Eq. (32) with Eq. (33), the flow area of every fracture, A_i (i = 1,2, … ,n), their shapes, and locations are then determined.
Step 7: Through definite integral, the intersecting areas are obtained. Thereafter, the actual production rates of every fracture and horizontal well are obtained.
Step 8: Substituting the actual production rates of every fracture with Eq. (25), the bottom-hole pressure of every fracture and the distribution of pressure in a horizontal wellbore are also acquired.

4. Field example

In order for it to be easy to verify the results, the three horizontal wells, namely, the Well WH1, the Well WH2, and the Well WH3 have been selected as well examples because there are exists data on the interpretation results and monitored fracture data in these particular wells. Their fracture stages are 3, 4, and 5, respectively. The Well WH1 had three stages and a 1103 m-horizontal well length that was analyzed in detail. The control range of the Well WH1 in the well pattern is 1600 m × 600 m, and the other data are shown in Tables 1 and 2.

Whenever $P_{wf} = 0.1$ MPa, the interference between adjacent fractures and horizontal wellbore friction (HWF) are considered, the production rates of the three fractures are $Q_{sc1} = 19.33 \times 10^4$ m^3/d, $Q_{sc2} = 18.99 \times 10^4$ m^3/d, and $Q_{sc3} = 1.39 \times 10^4$ m^3/d, respectively; the open-flow capacity of this well is Q_{AOF}, is 39.71×10^4 m^3/d. Whenever HWF is not considered, the open-flow capacity of this well is 42.34×10^4 m^3/d. Meanwhile, the open-flow capacity of this well evaluated by pressure buildup testing data and Topaze well test analysis software is 40.72×10^4 m^3/d, which is closer to the result that considers friction; in addition, the relative error is −2.49%.

The flow rates of the well, every fracture, and the distribution of pressure in the horizontal wellbore are calculated under different bottom-hole pressures (0.1 MPa, 1 MPa, 5 MPa, 10 MPa, 15 MPa, and 20 MPa) (Table 3 and Fig. 5).

Table 3 shows that the production rates of fractures increase from toe to heel of the horizontal well whenever the HWF is considered. Fig. 6 indicates that the flow area and production rate of fracture No. 3 decreases evidently because of the spacing between fracture No. 2 and No. 3. The reservoir near the toe of the well is invalid, and there is no fracturing. Therefore, there is no production contribution, and the bottom-hole pressure in fracture No. 3 is higher in Fig. 6.

Table 1
Basic parameters of the Well WH1.

Temperature (T)/K	Original pressure (P_i)/MPa	Formation permeability (k)/($\times 10^{-3}$μm^2)	Gas viscosity (μ)/(mPa.s)	Gas deviation factor (Z)	Gas relative density (γ_g)	Radius of horizontal wellbore (r_w)/m	Roughness of wellbore wall(e)/mm
385	31.7	0.74	0.023	0.98	0.598	0.076	3

Table 2
Fractures parameters of the Well WH1.

No.	Half-length (x_f)/m	Permeability (k_f)/($\times 10^{-3}$μm^2)	Width/(w_f)/m	Height/(h)/m	Spacing/(d)/m	Semi-major axis (a)/m	Semi-minor axis (b)/m
1	70	5000	0.01	12	143	220	208
2	40	4500	0.01	10	310	133	127
3	30	3500	0.01	9	38	100	96

Table 3
Production of each fracture in the WH1 under various bottom-hole pressures.

P_{wf}/MPa/	Q_{sc1}/($\times 10^4$ m^3/d)	Q_{sc2}/($\times 10^4$ m^3/d)	Q_{sc3}/($\times 10^4$ m^3/d)	Q_{avg}/($\times 10^4$ m^3/d)	Variance
0.1	19.33	18.99	1.39	13.24	70.19
1	19.31	18.97	1.39	13.22	70.03
5	18.87	18.55	1.36	12.93	66.91
10	17.49	17.22	1.26	11.99	57.58
15	15.17	14.97	1.09	10.41	43.44
20	11.87	11.75	0.86	8.16	26.65

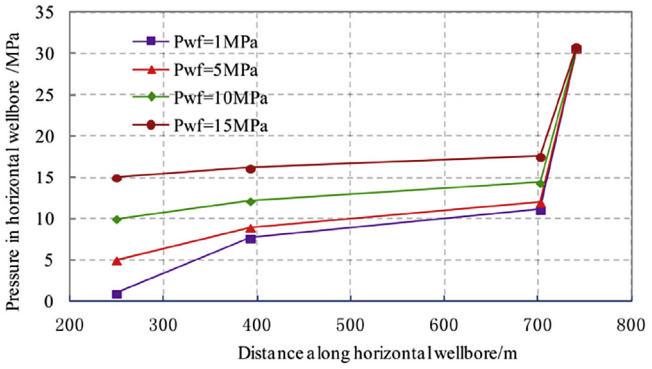

Fig. 5. Distribution of pressure in horizontal wellbore under various bottom-hole pressures.

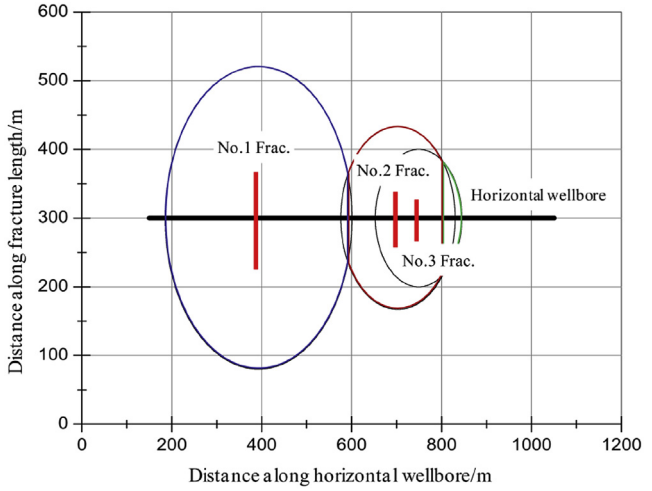

Fig. 6. Discharge area of fractures in Well WH1 when considering interference between adjacent fractures.

Table 6
Q_{AOF} of the Well WH2 and the Well WH3 as well as production of every fracture where $P_{wf} = 0.1$ MPa.

Well name	Production rate of every fracture/($\times 10^4$ m^3/d)					Open flow rate of well/($\times 10^4$ m^3/d)		
	No. 1	No. 2	No. 3	No. 4	No. 5	This results	Well testing results	Relative error/%
WH2	11.48	9.09	8.10	10.37		39.04	36.91	5.8
WH3	5.83	5.74	5.85	4.85	6.17	28.44	25.92	9.7

In addition, the primary basic and fractures parameters of the Well WH2 and the Well WH3 is shown in Tables 4 and 5. Their other parameters are the same to that of the Well WH1. It is consistent with calculated open flow rates with that of well-testing interpretation (Table 6).

5. Conclusions

Based on the basic flow principle within porous media, the whole flow process undergoes three stages according to the gas flow path from the matrix to hydraulic fracture, and lastly to the horizontal wellbore. The laws of variable flow in every part of the three stages are analyzed. Finally, we have presented a practical analytical model and analyzed three well examples of a tight gas reservoir. The following conclusions are warranted from the work presented in this paper:

(1) A single fracture segment is a unit, and all fracture sections are coupled by variable flow in a horizontal wellbore. Moreover, the effect of the interference between adjacent fractures on production and pressure of every fracture is

Table 4
Basic parameters of the Well WH2 and the Well WH3.

Well WH2				Well WH3			
Temperature (T)/K	Original pressure (P_i)/MPa	Formation permeability (k)/($\times 10^{-3}$μm^2)	Horizontal well length (L)/m	Temperature (T)/K	Original pressure (P_i)/MPa	Formation permeability (k)/($\times 10^{-3}$μm^2)	Horizontal well length(L)/m
387.8	30.5	0.51	505	389	31.3	0.35	969

Table 5
Fractures parameters of the Well WH2 and the Well WH3.

Well name	No.	Half-length (x_f)/m	Permeability (k_f)/($\times 10^{-3}$μm^2)	Height/ (h)/m	Spacing/ (d)/m	Semi-major axis (a)/m	Semi-minor axis (b)/m
WH2	1	30	3500	11	65	100.2	95.7
	2	30	3500	10	135	100.4	95.8
	3	30	3500	9	100	100.3	95.7
	4	30	3500	7	105	100.0	95.5
WH3	1	30	1000	8	50	97.6	92.9
	2	30	1000	8	120	99.6	95.0
	3	55	1500	8	255	180.6	172.0
	4	50	1500	8	185	164.7	156.9
	5	50	1500	8	210	161.7	153.8

evaluated quantitatively according to the principle of flow area. Thus, the new equations of predicting productivity are established and the method of solving the equations and its process are given.

(2) The open flow rates of three actual gas wells were calculated through the application of the equations, which conforms to the result of the well test evaluation. Additionally, we also quantitatively evaluated the contribution and effect of every fracture, thus, providing the theoretical basis for further optimization of the fracturing design.

(3) The method is suitable for predicting productivity of horizontal wells with non-uniform fracture system. That is unequal fracture spacing and fracture layout form, which is in line with the reality of complicated fracture system present in tight gas reservoirs. Meanwhile, it can also analyze the main factors influencing well productivity. Hence, the new method in this paper has broader prospects on predicting productivity of a multi-stage fractured horizontal well in the gas reservoir.

Foundation item

Supported by China Natural Science and Technology Major Project (2011ZX05015).

Conflict of interest

The authors declare no conflict of interest.

Acknowledgments

The authors wish to extend his sincere thanks to Changqing Oil Field, PetroChina and their colleagues for their help.

Nomenclature

P_D	dimensionless pressure
q_D	dimensionless fracture production
j_D	dimensionless length
C_{fD}	dimensionless fracture conductivity
P_i	original reservoir pressure, MPa
P	reservoir pressure, MPa
T	reservoir temperature, K
k	reservoir permeability, $\times 10^{-3}\mu m^2$
h	effective reservoir thickness, m
μ	gas viscosity, mPa·s
Z	gas deviation factor
Q_{sc}	fracture production under standard conditions, $\times 10^4$ m^3/d
q(x)	production of per unit length fracture under standard conditions, $\times 10^4$ $m^3/d/m$
x_f	fracture half-length, m
k_f	fracture permeability, $\times 10^{-3}\mu m^2$
w_f	fracture width, m
d	fracture spacing, m
r_w	horizontal wellbore radius, m
e	roughness on horizontal wellbore wall, mm
γ_g	gas relative density
f	friction resistance coefficient
R_{ei}	Reynolds number

References

[1] M. Parts, Effect of vertical fractures on reservoir behavior-incompressible fluid case, Soc. Pet. Eng. J. 1 (2) (1961) 105−118.
[2] H. Cinco-Ley, N. Dominguez, Transient pressure behavior for a well with a finite-conductivity vertical fracture, Soc. Pet. Eng. J. 18 (4) (1978) 253−264.
[3] Y.Z. Liao, W.J. Lee, New solutions for wells with finite-conductivity fractures including wellbore storage and fracture-face skin, in: SPE East Regional Meeting, 2−4 November, Pittsburgh, Pennsylvania, SPE 26912, 1993.
[4] A. Zerzar, Y. Bettam, Interpretation of multiple hydraulically fractured horizontal wells in closed systems, in: SPE International Improved Oil Recovery Conference in Asia Pacific, 20−21 October, Kuala Lumpur, Malaysia. SPE 84888, 2003.
[5] M. Brown, E. Ozkan, R. Raghavan, H. Kazemi, Practical solutions for pressure transient responses of fractured horizontal wells in unconventional reservoirs, in: SPE Annual Technical Conference and Exhibition, 4−7 October, New Orleans, Louisiana. SPE 125043, 2009.
[6] S.D. Joshi, Argumentation of well productivity with slant and horizontal wells, J. Pet. Technol. 8 (6) (1988) 729−739.
[7] S.D. Joshi, Production forecasting methods for horizontal wells, in: International Meeting on Petroleum Engineering, 1−4 November, Tianjin, China. SPE 17580, 1988.
[8] R. Raghavan, S.D. Joshi, Productivity of multiple drainholes or fractured horizontal wells, SPE Form. Eval. 8 (1) (1993) 1−16.
[9] X.D. Wang, G.H. Li, F. Wang, Productivity analysis of horizontal wells intercepted by multiple finite-conductivity fractures, Pet. Sci. 7 (2010) 367−371.
[10] Wang Junlei, Jia Ailin, He Dongbo, Wei Yunsheng, Qi Yadong, Rate decline of multiple fractured horizontal well and influence factors on productivity in tight gas reservoirs, Nat. Gas Geosci. 25 (2) (2014) 278−285.
[11] Bo Li, Jia Ailin, He Dongbo, Zhikai Lü, Bo Ning, Guang Ji, Productivity evaluation of horizontal wells in Sulige tight gas reservoir with strong heterogeneity, Nat. Gas Geosci. 26 (3) (2015) 539−549.
[12] Li Qin, Chen Cheng, Xun Xiaoquan, A new method of predicting gas wells' productivity of fractured horizontal well of low-permeability tight gas reservoir, Nat. Gas Geosci. 24 (3) (2013) 633−638.
[13] Wei Yunsheng, Jia Ailin, He Dongbo, Guang Ji, A new way of evaluation productivity of staged fracturing horizontal well in tight gas reservoir, Drill. Prod. Technol. 35 (1) (2012) 32−34.
[14] Shilun Li, Natural Gas Engineering, Petroleum Industry Press, Beijing, 2008, pp. 1−397.
[15] Mingqiang Hao, Yongle Hu, Fanhua Li, Production decline laws of fractured horizontal wells in ultra-low permeability reservoirs, Acta Pet. Sin. 33 (2) (2012) 269−273.
[16] Yanbo Xu, Tao Qi, Yang Fengbo, Huaiyin Li, Shouxin Zhou, New model for productivity test of horizontal well after hydraulic fracturing, Acta Pet. Sin. 27 (1) (2006) 89−91.
[17] M.F. Riley, W.E. Brigham, R.N. Horne, Analytic solutions for elliptical finite-conductivity fractures, in: SPE Annual Technical Conference and Exhibition, 6−9 October, Dallas, Texas, SPE 22656, 1991.
[18] M. Prats, P. Hazebroek, W.R. Strickler, Effect of vertical fractures on reservoir behavior: compressible-fluid case, Soc. Pet. Eng. J. 2 (2) (1962) 87−94.

[19] Wang Xiaodong, Zhang Yitang, Liu Ciqun, Productivity evaluation and conductivity optimization for vertically fractured wells, Pet. Explor. Dev. 31 (6) (2004) 78−81.

[20] Tongyu Yao, Weiyao Zhu, Jishan Li, Ming Wang, Fracture mutual interference and fracture propagation roles in production of horizontal gas wells in fractured reservoir, J. Cent. South Univ. Sci. Technol. 44 (4) (2013) 1487−1492.

[21] Jia Deng, Weiyao Zhu, Qian Ma, A new seepage model for shale gas reservoir and productivity analysis of fractured well, Fuel 124 (2014) 232−240.